Geoderma 473 (2026) 117966

Contents lists available at ScienceDirect

Geoderma

journal homepage: www.elsevier.com/locate/geoderma

Wheat genotypic variation in root architecture modifies soil pore structure and hydraulic properties

Bartolo Giuseppe Dimattia [a,*], Marco Bittelli [a], Fausto Tomei [b], Roberto Tuberosa [a], Maria C. Hernandez-Soriano [c]

[a] Department of Agricultural and Food Sciences, University of Bologna, Viale Fanin 44, 40125 Bologna, Italy
[b] Regional Agency for Environmental Protection and Energy, Emilia-Romagna Region, Viale Silvani 6, 40122 Bologna, Italy
[c] John Innes Centre, Norwich Research Park, Norwich NR4 7UH, United Kingdom

ARTICLE INFO

Handling Editor: Dr. H Neely

Keywords:
Wheat genotypes
Root-soil interactions
Pore connectivity
Hydraulic conductivity
Water retention

ABSTRACT

Root-driven modification of soil hydraulic properties may influence crop water availability and resilience under climatic variability, yet genotype-specific effects on rhizosphere hydrology remain poorly understood.

This study examined how contrasting root architectures of four wheat genotypes, two modern cultivars (Paragon, Bologna) and two landraces (Watkins 238, Senatore Cappelli), modify soil hydraulic behaviour under field conditions. Baseline (pre-sowing), bulk (fallow), and rhizosphere soils were characterised for water retention, unsaturated hydraulic conductivity, and pore size distributions derived from fitted retention curves. Root morphological traits were quantified using crown imaging and root scanning.

Genotypes differed markedly in both root traits and their associated hydraulic responses. Paragon, Watkins 238, and Senatore Cappelli exhibited bimodal pore size distributions, characterised by two peaks in the pore radius probability density function, whereas Bologna, baseline, and bulk soil displayed unimodal behaviour with a single dominant pore domain. Watkins 238 achieved the most significant improvement in hydraulic properties, increasing plant-available water to 0.21 $m^3\ m^{-3}$ (vs. 0.15 $m^3\ m^{-3}$ in baseline), driven by a lower permanent wilting point (0.12 $m^3\ m^{-3}$) and higher field capacity (0.34 $m^3\ m^{-3}$). Watkins 238 also displayed higher unsaturated conductivity, with hydraulic conductivity at field capacity and wilting point significantly higher than baseline and Bologna, and an area under the K(ψ) curve of 46.1, more than double that of other genotypes.

Root network area, root diameter, and branching frequency were significantly correlated with water retention parameters and conductivity metrics ($p < 0.05$ to $p < 0.001$), indicating that root systems reshape the pore network and soil hydrological properties. These findings suggest genotype-specific modification of hydraulic processes and highlight opportunities to leverage root traits to enhance water availability and resilience under water-limited conditions.

1. Introduction

Soil health underpins agricultural productivity and resilience to climate variability, with the regulation of water availability being a central function (Bronick and Lal, 2005; Doran and Parkin, 2015). This regulation is governed by soil structure and pore network connectivity, which control water infiltration, retention, and redistribution through the soil matrix (Dexter, 2004; Young and Ritz, 2005; Rabot et al., 2018). These physical attributes strongly influence plant water supply and susceptibility to erosion or waterlogging (Bordoloi et al., 2019).

Soil hydraulic properties provide a quantitative framework for describing water retention and flow. Advances in measurement and modelling now enable improved characterisation of pore-scale processes and hydraulic behaviour (Bezerra-Coelho et al., 2018). Soil hydraulic properties are governed by soil pore architecture and mediate water retention and transport; in vegetated systems, roots and associated biota modify pore networks, thereby altering hydraulic behaviour (Lu et al., 2020).

Water retention and flow in unsaturated soils depend on the relationship between water content, water potential, and hydraulic conductivity (Bittelli et al., 2015). These hydraulic properties determine how water is stored, transmitted, and made available to plants and are

* Corresponding author.
E-mail address: bartolo.dimattia2@unibo.it (B.G. Dimattia).

https://doi.org/10.1016/j.geoderma.2026.117966
Received 10 June 2025; Received in revised form 18 July 2026; Accepted 27 July 2026
Available online 31 July 2026

therefore closely linked to crop performance and drought resilience. Because root growth can modify soil pore architecture and connectivity, changes in root system architecture may influence hydraulic behaviour and alter water availability in the rhizosphere (Lu et al., 2020). Understanding these root-mediated hydraulic responses is therefore important for linking plant traits with soil physical functioning under field conditions.

Root systems play a central role in shaping soil structure and hydraulic properties by influencing soil aggregation (Hallett et al., 2022), pore formation and connectivity (Bengough et al., 2011), and water flow through mechanical and biochemical interactions with the surrounding soil matrix (Gregory, 2006; Lynch, 1995). Through growth, turnover, and interactions with the soil matrix, roots drive soil structural evolution and exhibit substantial complexity and plasticity, reflecting adaptation to heterogeneous soil environments (Hodge et al., 2009; Grossman and Rice, 2012). Beyond enabling anchorage, resource uptake, and carbohydrate storage (Evert, 2006), roots act as ecosystem engineers, exerting mechanical forces, depositing organic compounds, and altering pore continuity as they explore the soil. This architectural plasticity supports plant responsiveness to biotic and abiotic stresses (Bardgett et al., 2014), thereby reshaping pore architecture and water flow pathways. Advancing our understanding of root–soil interactions and their consequences for soil structure is therefore critical for enhancing soil hydraulic functionality and supporting long-term agricultural sustainability (Dexter, 2004).

The rhizosphere, defined here as the zone of soil directly influenced by root growth, exudation, and associated biological and physical processes, is a dynamic interface where root activity can modify soil structure and hydraulic behaviour (Wang et al., 2022). During growth, roots mechanically rearrange soil particles and modify pore architecture by creating new macropores through penetration, altering the size distribution and connectivity of existing pores, and occasionally occluding pores depending on root diameter and branching patterns (Bengough et al., 2011; Jin et al., 2013; Bodner et al., 2014; Lu et al., 2020). Root activity also affects soil aggregation. Macroaggregates may fragment within the rhizosphere while microaggregates form through the binding effects of root exudates and associated microbial activity (Hallett et al., 2022). These structural changes influence soil hydraulic properties, including infiltration, water retention, permeability, and aeration (Bronick and Lal, 2005). After root senescence, decomposing roots generate biopores that increase macroporosity and create preferential flow pathways, extending the influence of root systems on soil structure and hydrological processes beyond the growing season (Carminati and Vetterlein, 2013; Bodner et al., 2014).

While interspecific differences in root–soil interactions have been explored (Helliwell et al., 2017; Staszel-Szlachta et al., 2024), emerging evidence indicates that genotypes within a single crop species can also differ in their capacity to alter pore structure (Koebernick et al., 2019; Lucas et al., 2019; Zhou et al., 2021). In wheat, documented genotypic variation in root system architecture (RSA) and rhizodeposition suggests the potential for divergent impacts on soil physical properties (Bodner et al., 2014; White et al., 2015; Corneo et al., 2016; Fradgley et al., 2020). Wheat landraces preserve root architectural diversity that was substantially reduced during modern cultivar selection (Wingen et al., 2014). Including landraces and modern cultivars in this study allowed us to test whether landrace-derived root variation translates into measurable rhizosphere hydraulic benefits in a contemporary field setting.

While the effects of agricultural management on soil hydraulic properties are well documented (Blanco-Canqui et al., 2007; Strudley et al., 2008), root-induced modifications remain challenging to quantify, particularly under field conditions and at larger spatial scales. This difficulty arises because root morphological traits, including diameter, density, and architectural configuration, can have contrasting effects on water retention and hydraulic conductivity depending on soil texture, moisture conditions, and the stage of root development or decay (Carminati et al., 2016; Lu et al., 2020).

However, quantifying root architecture under field conditions is essential for understanding its influence on soil physical processes, as field-based phenotyping approaches provide realistic measures of root system expression and spatial organisation (Trachsel et al., 2011).

Building on our previous work demonstrating that wheat genotypes differ in root morphology and rhizosphere pore structure, as revealed by X-ray computed tomography (Dimattia et al., 2025), the objective of this study was to determine whether these previously observed structural differences translate into measurable differences in soil hydraulic properties.

We hypothesised that:

(i) previously identified genotype-dependent differences in root architecture and pore organisation would result in measurable differences in water retention, pore size distribution, and unsaturated hydraulic conductivity relative to bulk and baseline soils; and (ii) specific root morphological traits, including root diameter, branching frequency, and root system extent, would be significantly associated with key hydraulic parameters, indicating trait-mediated modification of rhizosphere hydraulic function.

To address these hypotheses, we analysed root architecture of four wheat genotypes with contrasting root phenotypes and characterised the hydraulic properties of their rhizosphere soils to identify relationships between root traits and soil hydraulic behaviour.

2. Materials and methods

2.1. Field trial and wheat genotypes

The field experiment was conducted at the DISTAL experimental farm (Department of Agricultural and Food Sciences, University of Bologna) in Cadriano (Bologna, Italy; 44.5491° N, 11.4130° E). The climate is subhumid, characterised by a mean annual temperature of 12.8 °C and an average annual precipitation of 924 mm.

Baseline physical and chemical soil properties were characterised prior to the experiment (Supplementary Table 1). The soil at the site is classified as a loam according to the USDA textural classification, based on particle size analysis. The field experiment was established as a randomised complete block design with three independent field replicates plots per genotype (n = 3). Each plot covered 6 m^2 and represented the experimental unit for subsequent soil hydraulic analyses. In addition to genotype-specific rhizosphere samples, reference soils consisted of three baseline soil replicates collected prior to sowing (n = 3) and three bulk soil replicates collected during the growing season from inter-row areas minimally influenced by roots (n = 3). Seeds were sown on 26 November 2022 at a density of 23 g of seeds per m^2. The experimental field had not undergone tillage operations for the previous two years. During the growing season, nitrogen fertiliser was applied twice at a rate of 24 kg N ha^{-1} per application: first at the tillering stage (13 February 2023) and again at stem elongation (17 April 2023).

Four wheat genotypes were selected to evaluate the influence of root systems on soil hydraulic properties: Watkins 238 (bread wheat landrace), Paragon and Bologna (modern elite bread wheat cultivars), and Senatore Cappelli (durum wheat landrace). These genotypes represent phylogenetically distinct material from both hexaploid and tetraploid wheat collections (Wingen et al., 2014; Maccaferri et al., 2019). The selection was based on a preliminary screening of root morphology across 20 wheat genotypes (Dimattia et al., 2025), where principal component analysis identified these four genotypes to represent contrasting root phenotypes (Supplementary Fig. 1). The two modern bread-wheat cultivars (Paragon, Bologna) provide a within-class contrast between a large, thicker-rooted (Paragon) and a compact, fine-rooted (Bologna) phenotype, complemented by a Watkins bread-wheat landrace at the high-extent end of PC1 (Watkins 238) and a heritage durum landrace at the extreme of large, thick-rooted phenotypes (Senatore Cappelli).

2.2. Root characterization

One soil monolith (40 cm length × 30 cm depth) was excavated from each plot at the plants flowering stage, and the root systems were carefully washed to remove adhering soil. From each monolith, three healthy, representative plants were selected to represent the typical phenotype of the plot while excluding individuals with visible damage or disease. Individuals showing symptoms of biotic stress (e.g. pests or pathogens) or physical damage (e.g. lodging or mechanical injury) were excluded to minimise confounding factors unrelated to genotypic expression. This targeted selection follows common field sampling practices in root and rhizosphere studies, where destructive sampling limits the number of samples (Trachsel et al., 2011; York et al., 2018). Root crown imaging and individual root component scanning were conducted according to the methodology described by Dimattia et al. (2025). This protocol includes frontal and rotated image acquisition for root crown architecture and high-resolution scanning of seminal and nodal roots in water-filled chambers for detailed morphometric analysis. Representative images and the RhizoVision Explorer workflow used to extract architectural traits are shown in Supplementary Fig. S2.

Root image analysis was performed using RhizoVision Explorer, an established platform for quantitative characterisation of root traits (Seethepalli et al., 2021). The acquired images were analysed to quantify root architectural traits describing overall spatial occupation and orientation, including root network area, convex area, morphological fragmentation patterns, and root angle (shallow vs. steep) consistent with the framework of Le Marié et al. (2019). Scanned root components were analysed using the broken-root analysis to quantify dimensional and branching attributes, according to trait definitions commonly used in root phenotyping research (Freschet et al., 2021; Dimattia et al., 2025). Extracted metrics included total root length, diameter-class lengths (<0.45 mm and > 0.45 mm), average and maximum diameter, number of root tips and branching points, and branching frequency. Root morphology data for Paragon, Cappelli, and Watkins 238 were previously generated and reported in Dimattia et al. (2025) using plants collected from the same field experiment and sampling campaign. These previously characterised root traits were incorporated here to enable integration with the newly generated soil hydraulic measurements. Soil hydraulic measurements presented in the current study were obtained from independently collected undisturbed soil cores and therefore represent a separate dataset from the previously reported root and X-ray CT analyses.

2.3. Soil sampling and measurement of hydraulic properties

Undisturbed soil cores (inner diameter 8 cm, height 5 cm) were collected using stainless-steel sampling cylinders for soil hydraulic measurements. At the end of the growing season, one undisturbed soil core was collected from each field replicate plot for each genotype, at 10–15 cm depth from within the crop row to capture soil directly influenced by root growth and associated rhizosphere processes (hereafter referred to as rhizosphere soil), resulting in three independent hydraulic replicates per genotype (n = 3). To distinguish root-mediated hydraulic modifications from seasonal changes in soil physical conditions, one additional bulk-soil core was collected per block from the inter-row area at an equivalent depth (n = 3 total), representing soil minimally influenced by roots. Baseline soil hydraulic properties were determined from three independent soil cores collected before sowing (n = 3).

Soil water retention curves (SWRCs) were determined using the evaporation method (Wind, 1968) and the dew point potentiometer technique (Campbell et al., 2007). Saturated hydraulic conductivity was measured using the constant head method, a widely applied approach for core-scale saturated flow assessment (Klute and Dirksen, 2018). Unsaturated hydraulic conductivity (K) was derived by applying an inverse solution of Richard's equation to data obtained from the evaporation experiment, following the approach of Peters and Durner (2008).

Saturated hydraulic conductivity was determined on undisturbed soil cores using the constant-head permeameter method following the principles described by Klute and Dirksen (2018). Measurements were performed using a KSAT system (METER Group AG, Munich, Germany) under a constant hydraulic head of 5 cm. Prior to measurement, soil cores were saturated for 72 h to ensure complete filling of the pore space with water. Hydraulic conductivity (K_s) was measured three times for each soil core. The resulting values were normalised to a reference temperature of 10 °C to correct for the effect of water viscosity on flow rate. After the K_s measurements, the soil cores were re-saturated for 12–24 h to restore uniform hydration before soil water retention measurements using the evaporation method.

SWRCs and K from 0 to approximately 120 J kg^{-1} were determined using the HYPROP2 evaporation method (METER Group Inc., Pullman, WA, USA), following established evaporation-method procedures (Peters and Durner 2008; Schindler et al. 2010). During these measurements, the mass of the soil cores and the matric potential values were recorded every 10 min using two tensiometers installed at fixed depths within each 5 cm soil core (1.25 and 3.75 cm below the soil surface), following the standard HYPROP2 configuration. The analysis was terminated upon reaching the air entry point of the ceramic plates in the tensiometers (approximately 120 J kg^{-1}), following the HYPROP2 measurement protocol. At this stage, the entire sample, including the sampling cylinder, was weighed to determine its wet mass.

Upon completion of the HYPROP2 analysis, each soil core was vertically bisected and three subsamples were collected from the inner portion of the core exclusively to extend water retention measurements into the dry range using a dew point potentiometry (WP4C, METER Group Inc., USA) following Singh and Verdi (2024). These subsamples were collected as follows: one from the upper distal section (driest zone), one from the central section (intermediate moisture), and one from the lower distal section at the height of the smaller tensiometer (comparatively wetter zone). These subsamples were treated as technical subsamples for parameterisation rather than independent biological replicates.

This sampling strategy ensured that the three subsamples spanned a range of water potentials, providing distinct data points for curve fitting in the low-potential domain. Each subsample was sealed in the WP4C sample cup and allowed to equilibrate overnight before measurement; the instrument determines water potential by chilling a mirror to the dew point temperature of the headspace air in equilibrium with the sample, allowing determination of matric potential across a range of approximately − 0.1 to − 300 MPa. Gravimetric water content was subsequently determined by oven-drying all subsamples at 105.5 °C for 24 h; the dried material was then reintegrated with the remaining core to determine the total dry weight of the soil sample (Campbell et al., 2007).

2.4. Parameterisation of the unsaturated hydrological properties

Soil water retention curves were parameterised using the bimodal van Genuchten model (van Genuchten, 1980; Durner, 1994; Seki et al., 2022; Šimůnek et al, 2024), an extension of the original van Genuchten formulation that allows representation of soils exhibiting multimodal water retention behaviour.

$$S_e = \frac{\theta - \theta_r}{\theta_s - \theta_r} = \sum_{i=1}^{k} w_i \left[\frac{1}{[1 + (\alpha_i |\psi|)^{n_i}]^{m_i}} \right] \quad (1)$$

where S_e [-] is the effective degree of saturation, θ [m^3 m^{-3}] is the water content, θ_s [m^3 m^{-3}] is the saturated water content, θ_r [m^3 m^{-3}] is the residual water content, ψ[J kg^{-1}] is the matric potential, α_i is the inverse of the air-entry potential [kg J^{-1}], and n_i [-] and m_i [-] are dimensionless shape parameters controlling the steepness and curvature of the

retention function. Following the standard van Genuchten-Mualem formulation, m_i was constrained as $m_i = 1–1/n_i$. The parameter w_i [-] represents the weighting coefficient of each pore domain, and k [-] indicates the number of pore domains included in the model (Durner, 1994).

Field capacity (FC) and permanent wilting point (PWP) were computed from the soil water retention curve as:

$$FC = \theta(\psi = 33 Jkg^{-1})$$

$$PWP = \theta(\psi = 1500 Jkg^{-1})$$

Plant-available water (PAW) was then calculated as

$$PAW = Fc - PWP$$

Soil water potential is reported in absolute values in this study to facilitate curve-fitting procedures and graphical representation on logarithmic scales. Further details on parameter interpretation can be found in Durner (1994) and van Genuchten et al. (1992).

Unsaturated hydraulic conductivity was estimated from the fitted soil water retention curves using the Mualem–van Genuchten formulation (Mualem, 1976; van Genuchten, 1980; Schaap and van Genuchten, 2006) as implemented by Bittelli et al. (2015), adapted for bimodal parameterisation, where the same weighting factors w_0 and w_1 obtained from the retention model represent the relative contribution of each pore domain to hydraulic flow (Eq. (2). The bimodal water retention model and the corresponding bimodal Mualem–van Genuchten conductivity model are referred to collectively hereafter as the bimodal van Genuchten–Mualem model, and the parameters derived from this framework (θ_s, α_1, α_2, n_1, n_2, w_0, w_1, K_s, K_FC, K_WP, and the slope of the conductivity curve) as bimodal van Genuchten–Mualem hydraulic parameters. This analysis was used to describe water transport behaviour across the measured range of matric potentials.

$$K(\psi) = K_s S_e(\psi)^r \left[\sum_{i=1}^{k} w_i \left(1 - \left(1 - S_i(\psi)^{1/m_i} \right)^{m_i} \right) \right]^r \quad (2)$$

where $K(\psi)$ is the unsaturated hydraulic conductivity [kg s m^{-3}], K_s is the saturated conductivity [kg s m^{-3}], τ is the tortuosity parameter, and r is a parameter determined by the model used for integration of the pore size distribution. Empirical parameters $l = 0.5$ and $r = 2$ were used, reflecting values commonly applied in hydraulic conductivity models and selected here to ensure comparability with previous studies and to reduce parameter uncertainty. Unsaturated hydraulic conductivity was estimated by applying the Mualem–van Genuchten model following the numerical procedure described in Bittelli et al. (2015). Further analyses of the SWRCs were carried out to evaluate model performance and hydraulic behaviour.

Separately from hydraulic conductivity estimation, fitted soil water retention curves (SWRCs) were used to derive secondary descriptors of soil hydraulic behaviour, including equivalent pore-size distributions and conductivity-based metrics. Equivalent pore radii were estimated using the capillary equation (Eq. (3), and probability density functions were calculated from cumulative pore distributions. This analysis provided a structural interpretation of hydraulic behaviour by relating matric potential to equivalent pore radii. Following parameterisation of the SWRC, matric potential values were converted to equivalent pore radii using the capillary equation (Eq. (3), which relates matric potential to pore size under capillary equilibrium (Tuller et al., 1999).

$$r_c = \frac{2\gamma cos\beta}{\rho_l \psi_m} \quad (3)$$

In Eq. (3), r_c is the equivalent pore radius (m), γ is the surface tension of water (0.072 N m^{-1}), ρ_l is the density of water (1000 kg m^{-3}), β is the contact angle (30°), and ψ_m is the soil matric potential (J kg^{-1}). Constant values were selected following typical values for soils (Bittelli et al., 2015).

The cumulative pore radius distribution obtained from Eq. (3) was numerically differentiated using a five-point Lagrange polynomial scheme to derive the pore-size probability density function (PDF) (Burden and Faires, 1997; Bittelli et al., 2015). For bimodal distributions, two peaks were identified in the PDF.

The bimodal van Genuchten model was fitted independently for each soil core corresponding to an individual field replicate plot. The resulting hydraulic parameters were therefore estimated separately for each biological replicate and subsequently used for genotype comparisons. The resulting parameter estimates were used as independent experimental units for genotype comparisons to avoid pseudoreplication.

Two additional metrics were calculated to characterise hydraulic conductivity across the plant-available water range. First, the slope of the log(K)–log(ψ) relationship between field capacity (FC) and permanent wilting point (PWP) was calculated to quantify the rate at which hydraulic conductivity declines during soil drying (Ahuja et al., 1985; Rawls et al., 1998). Second, the area under the predicted K(ψ) curve (AUC) was calculated using trapezoidal integration to provide an integrated measure of unsaturated hydraulic conductivity across the same range of matric potentials (Alexander and Skaggs, 1986). Hydraulic conductivity values were extracted at two agronomically relevant matric potentials: field capacity (KFC; K evaluated at field capacity) and permanent wilting point (KWP; K evaluated at permanent wilting point). Together, AUC and slope summarise the overall behaviour of conductivity during soil drying.

2.5. Statistical analysis

Data normality was evaluated using the Shapiro-Wilk test and QQ plots. Statistical analyses were conducted using biological field replicates as the experimental units (n = 3 plots per genotype), with each soil core representing one independent observation for soil hydraulic analyses. Additional subsamples collected during WP4C measurements were used exclusively to extend the soil water retention curves into the dry range and were not treated as independent observations in statistical analyses.

To satisfy normality assumptions and stabilise variance, hydraulic parameters derived from soil water retention and conductivity analysis were log10-transformed prior to analysis. Specifically, transformations were applied to saturated water content (θs), van Genuchten shape parameters (α_1, α_2, n_1, n_2), saturated hydraulic conductivity (K_s), hydraulic conductivity at field capacity (KFC), hydraulic conductivity at permanent wilting point (KWP), the slope of the conductivity function, and the area under the conductivity curve (AUC). For simplicity, these variables are referred to without the log prefix throughout the text. In contrast, volumetric water content parameters (FC, PWP, PAW) and weighting coefficients (w_0, w_1) were analysed on their original scale because they vary within a narrow numerical range and satisfied parametric assumptions (Liu and Lennartz, 2019).

Differences among genotypes in soil hydraulic parameters and root phenotypic traits were assessed using one-way ANOVA, using field plots as the experimental units (n = 3 independent plots per genotype). One hydraulic soil core collected from each plot represented a single independent observation. Tukey's post-hoc test was applied only when the overall ANOVA indicated significant treatment effects. This statistical approach accommodates unequal group sizes, and bulk soil samples were included as a reference treatment rather than as a balanced factorial comparison with genotype-specific rhizosphere soils. Statistical significance levels were interpreted as $p < 0.01$ (highly significant), $p < 0.05$ (significant), and $p < 0.1$ (marginally significant), depending on the dataset and variability of the measured parameters.

Associations between root traits and soil hydraulic properties were examined using linear mixed models (LMMs), with the soil hydraulic parameter as the response, the root trait as a fixed-effect predictor, and

field plot as a random intercept.

3. Results

3.1. Wheat genotypes differed in root morphological and topological traits

Root traits of Paragon, Senatore Cappelli, and Watkins 238 were previously characterised under the same experimental conditions and described in detail by Dimattia et al. (2025). In the present study, we extend that dataset by including the Bologna genotype and integrating root architectural data with measurements of soil hydraulic properties to examine genotype-driven effects on rhizosphere hydrology. Significant variation among genotypes was observed across several root morphological and topological traits (Table 1). The following section provides a concise overview of the contrasting root phenotypes represented in this study as context for interpreting their associated hydraulic responses.

Overall, the four genotypes exhibited contrasting root architectures. Paragon developed the longest and most branched root system, with the coarsest root diameters. Senatore Cappelli had the largest whole-root area and fine, FRMP-rich roots. Watkins 238 also had fine roots and a high FRMP, but the lowest total root length, tip count, and branching of the panel. Bologna had the most compact whole-root architecture and intermediate-to-low broken-root values. Bologna also exhibited the smallest network area among the four genotypes ($p < 0.05$), the smallest convex area, and the lowest FRMP value (marginal at $p < 0.10$). At the individual-root scale, Watkins 238 displayed fewer branching points than Senatore Cappelli and Paragon ($p < 0.01$), lower branching frequency than Paragon ($p < 0.01$), and the shortest total root length ($p < 0.01$), together with the smallest root tip count ($p < 0.01$) and the shortest root length in both diameter classes (D1 < 0.45 mm: 1,170 mm vs 4,928 mm in Paragon, $p < 0.01$; D2 > 0.45 mm: 283 mm vs 1,157 mm in Paragon, $p < 0.01$). Bologna also differed significantly from Senatore Cappelli in the number of branching points ($p < 0.01$). Paragon developed the most extensive root system across nearly all topological metrics.

Table 1
Means ± standard error of root morphological and topological traits across four wheat genotypes. Data for Paragon, Senatore Cappelli, and Watkins 238 were previously reported in Dimattia et al. (2025). Different superscript letters within a row indicate significant pairwise differences among genotypes identified by Tukey's HSD post-hoc test (p < 0.05). Grouping letters are shown only for variables with significant overall ANOVA effects.

Root Trait	*p*-value	Paragon	Senatore Cappelli	Watkins 238	Bologna
	Whole root analysis				
Network area (mm2)	*	4435 ± 361^{ab}	5667 ± 391^{a}	4145 ± 454^{ab}	2359 ± 381^{b}
Convex area (mm2)	*	15002 ± 1460^{a}	16291 ± 2206^{a}	14714 ± 1659^{a}	11315 ± 1724^{b}
Shallow angle frequency	ns	0.22 ± 0.02	0.24 ± 0.01	0.23 ± 0.01	0.19 ± 0.02
Steep angle frequency	ns	0.51 ± 0.02	0.46 ± 0.01	0.48 ± 0.02	0.53 ± 0.02
[1]FRMP	†	451 ± 27	637 ± 86	636 ± 75	295 ± 51
	Broken root analysis				
Root tips	**	894 ± 127^{a}	506 ± 60^{a}	237 ± 45^{b}	434 ± 32^{a}
Total root length (mm)	**	6086 ± 828^{ab}	3200 ± 416^{a}	1353 ± 322^{b}	3479 ± 273^{a}
Root length D2 (> 0.45 mm)	**	1157 ± 100^{a}	546 ± 175^{b}	283 ± 42^{b}	524 ± 43^{b}
Root length D1 (< 0.45 mm)	**	4928 ± 734^{a}	2654 ± 743^{ab}	1170 ± 249^{b}	1954 ± 183^{b}
Branching points	**	3479 ± 612^{a}	1447 ± 189^{a}	635 ± 165^{b}	979.22 ± 98^{b}
Branching frequency (1/mm)	**	0.69 ± 0.08^{a}	0.35 ± 0.01^{b}	0.29 ± 0.03^{b}	0.34 ± 0.02^{b}
Max root diameter (mm)	*	1.93 ± 0.50^{a}	1.17 ± 0.13^{b}	1.19 ± 0.56^{b}	1.22 ± 0.34^{b}
Root diameter (mm)	*	0.93 ± 0.09^{ab}	0.56 ± 0.01^{b}	0.60 ± 0.02^{b}	0.76 ± 0.08^{a}

Significance based on one-way ANOVA: *$p < 0.05$, **$p < 0.01$, ***$p < 0.001$, † $0.05 \leq p < 0.10$, ns ≥ 0.10.
[1]FRMP: fragmented root morphological pattern, a descriptor of root system fragmentation and spatial distribution quantified according to Le Marié et al. (2019).

3.2. Rhizospheric hydraulic properties differ among the wheat genotypes

Significant differences were identified among soil samples for multiple parameters derived from the retention curves (Fig. 1a, Table 2). For visualisation purposes, retention curves were fitted using the pooled data from all replicates (Fig. 1b).

The bimodal van Genuchten equation accurately fitted the data (mean RMSE = 0.025 ± 0.015 J kg^{-1}), indicating consistency between the observed and modelled values throughout the entire range of matric potentials, with greater variability near saturation reflecting spatial heterogeneity among soil cores (Fig. 1a).

Watkins 238 displayed the highest saturated water content (θ_s), significantly above bulk soil (Tukey HSD, $p < 0.05$). The other rhizosphere soils were numerically higher than bulk soil but not statistically distinguishable from it. This pattern is consistent with increased effective water storage capacity and altered pore organisation in the Watkins 238 rhizosphere.

Watkins 238 displayed the smallest α_1 value, significantly lower than those of Bologna, Paragon, and baseline soil (Tukey HSD, $p < 0.05$ in all three contrasts). Senatore Cappelli and bulk soil also presented significantly lower α_1 values than Bologna and Paragon (Tukey HSD, $p < 0.05$). Bulk soil and baseline soil were not statistically distinguishable for this parameter. In the van Genuchten formulation, α represents the reciprocal of the air-entry value; therefore, lower α_1 values correspond to higher air-entry potentials and indicate the presence of smaller pores near saturation.

Watkins 238 also showed significantly higher n_1 values than Bologna ($p < 0.01$), Paragon ($p < 0.01$), and baseline soil ($p < 0.01$). No significant differences were observed among Senatore Cappelli, Paragon, and Watkins 238 for the secondary pore parameters α_2, n_2, and w_1, suggesting similar behaviour in the second pore domain. Comparisons with Bologna, baseline, and bulk soil were not possible for these parameters because their water retention curves did not exhibit bimodality.

Field capacity, permanent wilting point, and plant-available water differed significantly among treatments (Fig. 1, Table 2). Watkins 238 exhibited the highest FC (0.34 m^3 m^{-3}), significantly above baseline soil (0.27 m^3 m^{-3}; Tukey HSD, $p < 0.05$); the other rhizosphere soils (Paragon and Senatore Cappelli, both 0.32 m^3 m^{-3}; Bologna, 0.30 m^3 m^{-3}) were numerically higher than baseline but did not differ significantly from it. Watkins 238 also showed the lowest PWP (0.12 m^3 m^{-3} vs 0.16 m^3 m^{-3}, approximately − 25 %; Tukey HSD, $p < 0.05$), resulting in the highest PAW among all groups (0.21 m^3 m^{-3}), significantly exceeding baseline soil (0.15 m^3 m^{-3}), Paragon (0.16 m^3 m^{-3}), and Bologna (0.16 m^3 m^{-3}) by 40 %, 31 % and 31 %, respectively (Tukey HSD, $p < 0.05$ in all three contrasts). Senatore Cappelli showed intermediate PAW (0.19 m^3 m^{-3}), numerically higher than baseline but not statistically distinguishable from it. These genotypic differences in water retention across the plant-available water range are illustrated in Fig. 1.

Saturated hydraulic conductivity (K_s) differed significantly among treatments (Table 2). Rhizosphere soils associated with Paragon and Watkins 238 showed the highest K_s values (log K_s = 3.53 and 3.49, respectively), compared with baseline soil (2.66), bulk soil (3.01), and Senatore Cappelli (2.85). Bologna also exhibited higher K_s (3.26) than baseline soil. In contrast, Senatore Cappelli showed lower K_s than Bologna (Table 2).

Unsaturated hydraulic conductivity differed significantly among treatments (Table 2; Fig. 2). Watkins 238 maintained the highest

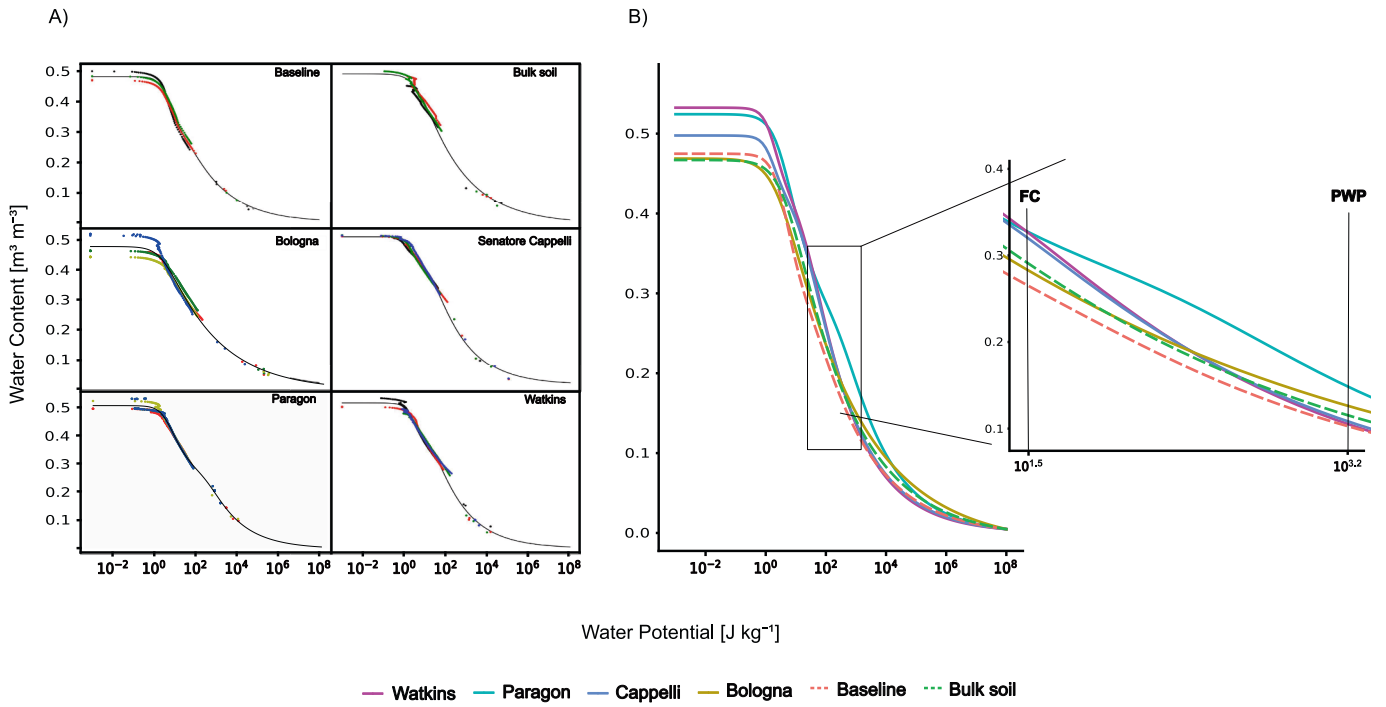

Fig. 1. Soil water retention curves for baseline soil, bulk soil, and rhizosphere soils associated with four wheat genotypes (Watkins 238, Paragon, Senatore Cappelli, and Bologna). Water potential is plotted as absolute values. **(A)** Soil water retention curves for each soil type showing measured volumetric water content (points) and fitted curves based on a modified bimodal van Genuchten model (lines). Grey lines represent individual replicate fits. **(B)** Comparison of the fitted retention curves for all treatments. The inset highlights the agronomically relevant range between field capacity (FC) and permanent wilting point (PWP).

Table 2
Values are means ± standard error of hydraulic properties of baseline, bulk, and genotype-specific rhizosphere soils derived from retention curves. Different superscript letters indicate significant differences among groups (Tukey HSD, $p < 0.05$). Dashes (—) indicate parameters not estimated due to unimodal retention behaviour. Grouping letters are shown only for parameters with a significant overall ANOVA effect.

Soil Parameter	p-value	Baseline	Bulk Soil	Paragon	Senatore Cappelli	Watkins 238	Bologna
log θs	***	−0.73 ± 0.03^{ab}	−0.81 ± 0.05^{b}	−0.66 ± 0.03^{ab}	−0.70 ± 0.01^{ab}	−0.64 ± 0.04^{a}	−0.75 ± 0.06^{ab}
log α1	***	−1.18 ± 0.04^{ab}	−3.41 ± 0.31^{bc}	−1.41 ± 0.66^{a}	−3.57 ± 0.11^{bc}	−4.75 ± 1.15^{c}	−1.00 ± 0.19^{a}
log α2	ns	–	–	−2.43 ± 2.79	−1.02 ± 0.11	−0.89 ± 0.42	–
log n1	***	0.18 ± 0.01^{b}	0.23 ± 0.01^{ab}	0.19 ± 0.03^{b}	0.27 ± 0.04^{ab}	0.36 ± 0.13^{a}	0.16 ± 0.01^{b}
log n2	ns	–	–	0.88 ± 0.39	0.53 ± 0.25	0.53 ± 0.19	–
log K_s	***	2.66 ± 0.11^{d}	3.01 ± 0.07^{bc}	3.53 ± 0.05^{a}	2.85 ± 0.15^{c}	3.49 ± 0.16^{a}	3.26 ± 0.07^{b}
w0	ns	1	1	0.87 ± 0.06	0.73 ± 0.04	0.64 ± 0.01	1
w1	ns	0	0	0.13 ± 0.06	0.26 ± 0.03	0.36 ± 0.01	0
FC	***	0.27 ± 0.01^{b}	0.31 ± 0.01^{ab}	0.32 ± 0.00^{ab}	0.32 ± 0.01^{ab}	0.34 ± 0.00^{a}	0.30 ± 0.01^{ab}
PWP	**	0.12 ± 0.00^{a}	0.13 ± 0.00^{ab}	0.16 ± 0.00^{a}	0.14 ± 0.01^{ab}	0.12 ± 0.01^{b}	0.14 ± 0.00^{ab}
PAW	***	0.15 ± 0.01^{c}	0.19 ± 0.00b^{c}	0.16 ± 0.00^{b}	0.19 ± 0.01b^{c}	0.21 ± 0.01^{a}	0.16 ± 0.01^{b}
log KFC	***	−5.78 ± 0.42^{c}	−3.73 ± 0.12^{b}	−4.68 ± 1.05^{ab}	−3.79 ± 0.41^{ab}	−2.72 ± 1.38^{a}	−5.57 ± 0.31^{c}
log KWP	***	−9.92 ± 0.47^{b}	−8.11 ± 0.13^{ab}	−8.85 ± 0.90^{ab}	−8.36 ± 0.52^{ab}	−7.29 ± 1.49^{a}	−9.60 ± 0.34^{b}
AUC	***	7.70 ± 1.45^{b}	24.96 ± 3.78^{b}	21.15 ± 6.87^{b}	21.06 ± 3.53^{b}	46.10 ± 16.20^{a}	10.70 ± 2.07^{b}
slope	***	−2.50 ± 0.04^{b}	−2.64 ± 0.02^{ab}	−2.51 ± 0.10^{b}	−2.76 ± 0.13^{a}	−2.76 ± 0.20^{a}	−2.43 ± 0.03^{b}

Significance based on one-way ANOVA: *$p < 0.1$, **$p < 0.05$, ***$p < 0.01$; ns, not significant. θ_s, saturated volumetric water content; α_1 and α_2, air-entry parameters for the macropore and micropore domains, respectively (lower α corresponds to a higher air-entry potential, i.e., smaller effective pore sizes); n_1 and n_2, shape parameters of the bimodal van Genuchten retention curve, related to the width of the pore-size distribution in each domain; w_0 and w_1, weighting factors representing the relative contribution of the macropore and micropore domains, respectively, to the bimodal retention curve; K_s, saturated hydraulic conductivity; KFC and KWP, unsaturated hydraulic conductivity at field capacity and at permanent wilting point, respectively; FC, field capacity (water content at − 33 kPa); PWP, permanent wilting point (water content at − 1500 kPa); PAW, plant-available water (FC − PWP); AUC, area under the hydraulic conductivity curve; slope, gradient of the log–log unsaturated hydraulic conductivity curve ($\Delta \log K / \Delta \log |\psi|$); more negative values indicate a more rapid decline of conductivity with drying, while values closer to zero indicate sustained conductivity at low matric potentials.

conductivity throughout the drying range, exhibiting the highest hydraulic conductivity at field capacity (KFC) and wilting point (KWP) and AUC values. In contrast, baseline soil and Bologna consistently showed the lowest conductivity metrics.

Although the slope of the log(K)–log(ψ) relationship was steeper (more negative) for Watkins 238 and Senatore Cappelli than for Bologna, Watkins 238 and Senatore Cappelli maintained higher K values throughout the drying range (Fig. 2), reflecting their higher saturation-end conductivity (K_s) and larger AUC. The flatter slope of Bologna therefore reflects a uniformly lower conductivity rather than greater sustained transmission. Senatore Cappelli showed lower K_s than Bologna but maintained higher unsaturated conductivity across the drying range, with greater KFC and a slope closer to zero, suggesting that the two genotypes modify soil hydraulic behaviour through distinct mechanisms.

Overall, Watkins 238 showed statistically significant higher values of

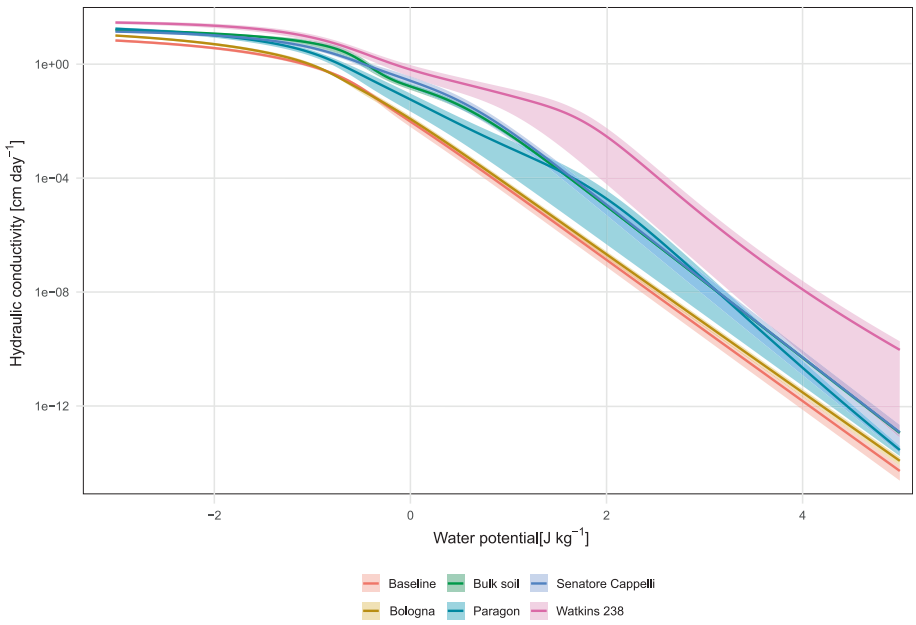

Fig. 2. Hydraulic conductivity (K) curves derived from bimodal van Genuchten–Mualem models fitted to soil water retention and conductivity data. Each line represents the mean log-transformed K(ψ) relationship for a given genotype or treatment, with shaded bands indicating the standard error across replicates.

K over the entire range of water potentials (Fig. 2), modifying the hydraulic behaviour of the original baseline soil and also with respect to the other genotypes.

3.3. Root architectural traits correlate with soil hydraulic properties

Linear mixed models revealed significant relationships between root morphology and hydraulic behaviour (Fig. 3). Root architectural traits primarily influenced water retention. Crown network area was positively associated with the macropore weighting factor w_0, field capacity, and plant available water, while FRMP was negatively related to α_1 but positively associated with θ_s, FC, and PAW ($p < 0.05$). Root angle distribution also affected pore-domain parameters, with shallow root angles associated with lower α_1 and n_2 and higher w_1, whereas steep root angles showed the opposite trend.

Traits related to root extent and topology (total root length, length in both diameter classes, and root tip number) exhibited similar relationships with hydraulic properties, being negatively associated with α_2, n_1, and saturated hydraulic conductivity (Ks), and positively associated with permanent wilting point (PWP). Branching frequency and root diameter were also significant predictors of hydraulic behaviour. Greater branching frequency was associated with reduced PAW, Ks, KFC, and KWP, but increased θ_s, α_1, PWP, and the conductivity-curve slope. Similarly, larger average root diameter was positively correlated with θ_s and α_1 but negatively with n_1, w_1, PAW, KFC, and KWP. Maximum root diameter showed a comparable pattern, being positively associated with n_2 and w_0 and negatively associated with n_1, w_1, and Ks.

3.4. Roots affect pore size distribution

Baseline and bulk soils exhibited unimodal distributions (Fig. 4) with peaks at 22.3 and 6.6 μm, respectively. Bologna, characterised by shorter, less branched roots, showed a unimodal distribution (peak at 9.9 μm) similar to bulk soil, with no significant effect on θ_s (Table 2), indicating limited influence on pore architecture.

In contrast, Paragon, Watkins 238, and Senatore Cappelli exhibited bimodal pore size distributions (Fig. 4). Paragon, which developed longer and thicker roots, produced a bimodal distribution with peaks at 17.3 μm (macropores) and 0.162 μm (micropores). This genotype also showed higher saturated water content (θ_s) than bulk soil ($p < 0.01$), indicating greater total porosity. Together, these results suggest that Paragon roots modified both the amount of pore space and its distribution within the rhizosphere.

Watkins 238 and Senatore Cappelli, characterised by finer, more elongated root systems, generated distinct bimodal distributions with larger macropore peaks (55.6 and 61.6 μm, respectively) and secondary micropore peaks around 2 μm.

4. Discussion

This study provides new evidence that genotypic variation in wheat root system architecture can modify soil hydraulic properties, including plant-available water (PAW), permanent wilting point (PWP), and hydraulic conductivity across saturation states. These findings support the idea that plant roots can actively modify soil structure and hydraulic properties through their growth and rhizosphere activity. Previous studies have shown that roots can change pore architecture and soil water dynamics by displacing soil particles and releasing organic compounds into the rhizosphere (Lu et al., 2020; Xiao et al., 2024). The observed differences among genotypes confirm that even within a single crop species, RSA traits shape the physical hydrology of the rhizosphere.

4.1. Root architecture as a driver of pore-scale hydraulic differentiation

In this study, genotypes with finer root diameters and architecturally complex root systems (high FRMP) were associated with greater water retention at lower matric potentials and lower α values, which in the bimodal van Genuchten parameterisation applied in this study correspond to smaller effective pore sizes and higher air-entry potentials (Bittelli et al., 2015). These results therefore suggest that root proliferation modified the rhizosphere pore architecture by increasing the proportion of smaller pores. Bologna and bulk soil exhibited unimodal retention curves, indicating a simpler pore architecture with less differentiation between macro- and micropore domains. This pattern is characteristic of soils with limited aggregation or reduced structural heterogeneity (Dexter, 2004; Jarvis, 2007) and consistent with the weaker rhizosphere restructuring expected from Bologna's compact root system. Paragon, Watkins 238 and Senatore Cappelli, by contrast, produced bimodal pore distributions consistent with the coexistence of inter-aggregate macropores and intra-aggregate micropores typical of

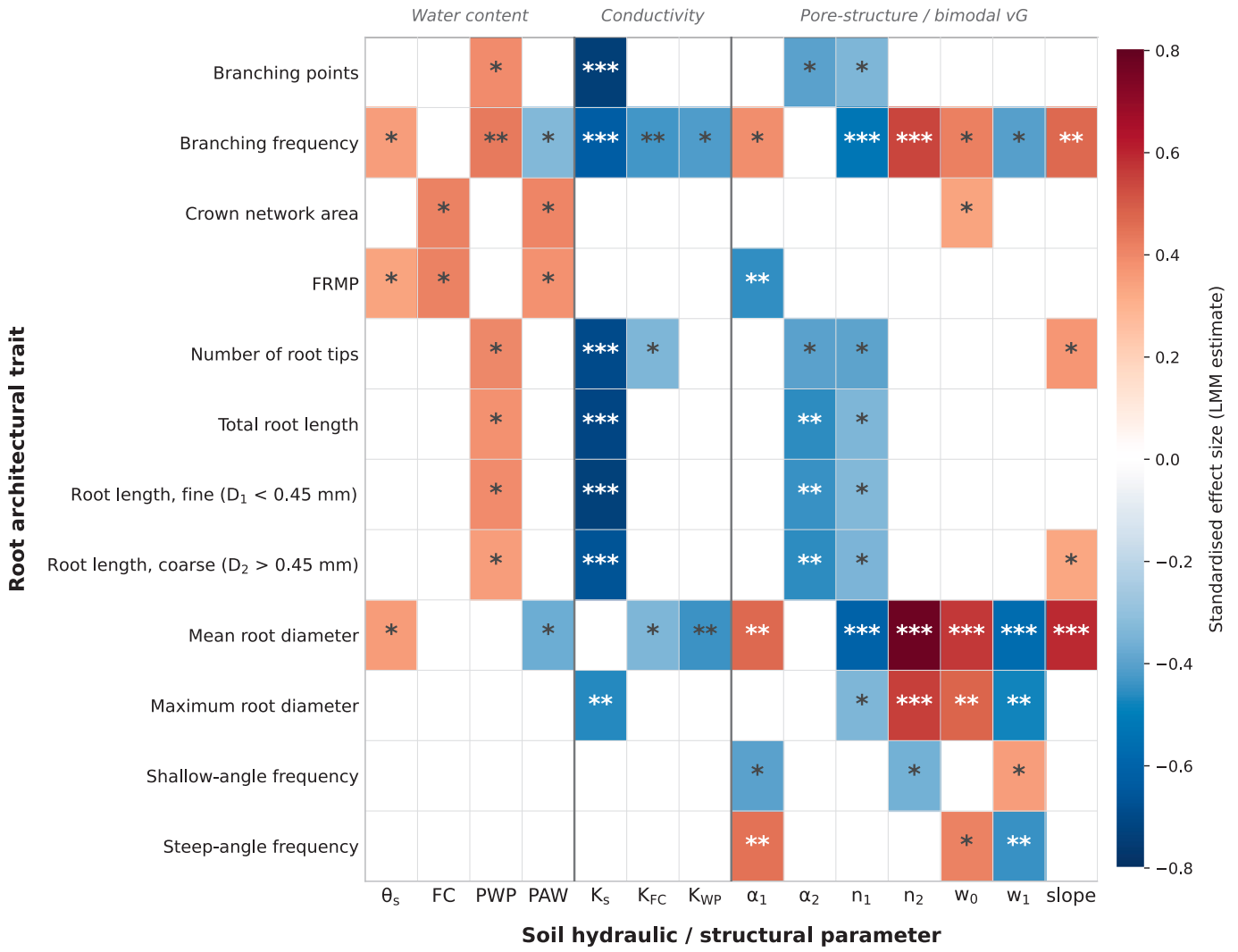

Fig. 3. Associations between root architectural traits and soil hydraulic and structural variables, estimated by linear mixed models with field plot as random intercept. Soil parameters are grouped by category along the horizontal axis as water content metrics: saturated water content (θ_s), field capacity (FC), permanent wilting point (PWP), and plant-available water (PAW); hydraulic conductivity metrics: saturated hydraulic conductivity (K_s), conductivity at field capacity (KFC), and conductivity at permanent wilting point (KWP); and parameters of the bimodal van Genuchten–Mualem model: air-entry parameters α_1 and α_2 for the macropore and micropore domains, pore-size distribution indices n_1 and n_2, weighting coefficients w_0 and w_1 that partition the dual-porosity contributions, and the slope of the unsaturated hydraulic conductivity curve. Root traits (vertical axis) are ordered by trait family: branching, crown architecture, root length, root diameter, and root angle distribution. Cell colour indicates the direction and magnitude of the standardised LMM effect estimate (blue, negative association; red, positive association), with colour intensity proportional to effect size as shown in the colour bar. Asterisks denote statistical significance: *, $p < 0.05$; **, $p < 0.01$; ***, $p < 0.001$. White cells indicate non-significant relationships ($p \geq 0.05$). FRMP, fragmented root morphological pattern; D_1, fine-root diameter class (< 0.45 mm); D_2, coarse-root diameter class (> 0.45 mm).

structured agricultural soils (Durner, 1994), potentially generated by root-induced aggregation or biopore formation after root decay. Our previous X-ray CT study on three of the same genotypes grown in this field showed that wheat cultivars differ markedly in their ability to restructure rhizosphere pore networks at both core and aggregate scales, generating persistent bioporosity that depends on root architecture, and that root traits correlated with pore network connectivity and biopore characteristics rather than with bulk pore volume alone (Dimattia et al., 2025). Genotypes can therefore generate pore systems of comparable size but differing topology, consistent with earlier X-ray CT observations of genotype-specific rhizosphere pore modification in soil columns for cover crops (Scholl et al., 2014) and wheat (Daly et al., 2015). In our study, the genotype Watkins 238 maintained the highest hydraulic conductivity at low matric potentials, suggesting that water flow was sustained through smaller, well-connected pores as the soil dried. Similar hydraulic responses have been described in fine-textured agricultural soils, where continuous micropore networks allow water movement even at low water potentials (Jarvis and Messing, 1995) and have been discussed more broadly in relation to water transport across contrasting soil textures (Marshall et al., 1996). These studies support the interpretation that the pore structure associated with Watkins 238 may promote hydraulic connectivity under drying conditions. These results reinforce the hypothesis that RSA determines hydraulic properties by influencing pore connectivity and tortuosity.

4.2. *Mechanisms underlying root–hydraulic interactions*

The trait–hydraulic associations identified (Fig. 3) and the genotypic contrasts described in Section 4.1 can be interpreted considering three non-exclusive mechanisms occurring in the rhizosphere: (i) mechanical restructuring of pore geometry, (ii) partial pore-filling that modifies connectivity, and (iii) rhizodeposit-mediated aggregation. Their relative contributions vary with root architecture, water potential, and soil texture. Mechanically, roots displace soil particles and modify pore

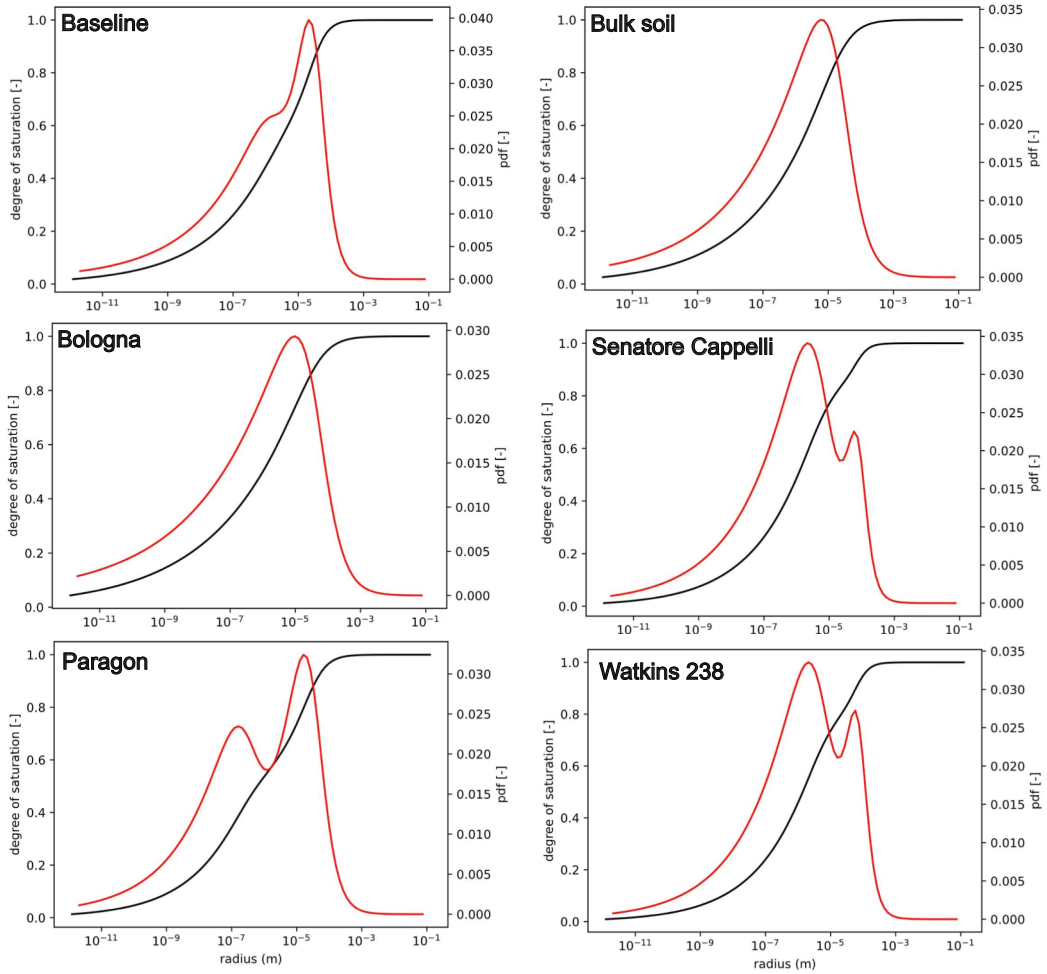

Fig. 4. Pore size distribution curves derived from soil water retention data using a capillary-based model. For each soil type (baseline, bulk, and rhizosphere) of the four wheat genotypes, panels display the differential water retention curve (black line) and the corresponding pore-radius probability density function (red line). Peaks in the probability density function indicate dominant pore domains, with single peaks reflecting unimodal pore structures and multiple peaks indicating bimodal or more heterogeneous pore-size distributions characteristic of rhizosphere modification.

geometry (Jin et al., 2017), and can partially fill existing pores, altering pore connectivity and hydraulic behaviour (Lu et al., 2020). In our loam soil, branching frequency and root tip number correlated negatively with K_s, KFC and KWP (Fig. 3), consistent with dense fine-root networks partially obstructing flow through medium-sized pores while maintaining connectivity in smaller pores. Fine-root proliferation may reduce water flow near saturation through partial pore clogging, while allowing sustained flow through micropores as soils dry (Hohenbrink et al., 2023). Mean and maximum root diameter showed the opposite pattern, with positive correlations with n_2, w_0 and the slope of the conductivity curve, indicating that thicker, more spatially distributed roots are more strongly associated with the macropore-domain structure that sustains flow during drying. These opposing trait signatures suggest that rhizosphere restructuring trades macropore conductivity for micropore continuity at high branching density (Hohenbrink et al., 2023), and that the observed increase in PWP without proportional gains in FC reflects a trade-off between total soil storage and plant-usable water that is itself trait-dependent. The Watkins 238 versus Senatore Cappelli contrast (comparable bimodal pore size distributions but markedly different K_s) further illustrates that this restructuring is ultimately governed by pore network topology rather than size composition alone (Dimattia et al., 2025; Jarvis, 2007). Bologna's compact root system, unimodal pore distribution, and uniformly lower hydraulic conductivity across the drying range (despite a flatter slope of − 2.43) define the opposite extreme of limited rhizosphere modification.

The third mechanism, not directly quantified here, is mucilage- and rhizodeposit-mediated aggregation. Mucilage enhances aggregate stability through its rheological properties (Naveed et al., 2019) and modifies pore-scale water retention (Holz et al., 2018) and connectivity (Kroener et al., 2018). Because mucilage is exuded primarily from root tips and elongation zones, the spatial extent of its stabilising influence scales with root tip density and total root surface area rather than with root volume. Paragon, with the highest branching frequency, root tip count, and total root length in the panel (Table 1) would therefore expose the largest soil volume to mucilage influence, consistent with its strongly developed bimodal pore structure and very fine micropore peak (0.162 μm). The thinner-rooted but lower-branching Watkins 238 and Senatore Cappelli would generate more spatially distributed but locally less abundant mucilage coverage, while Bologna's compact, low-branching system implies the smallest rhizosphere footprint. Because mucilage hydrophilicity declines on drying (Carminati et al., 2010; Hallett and Young, 1999) and our measurements extend to PWP, mechanical restructuring and connectivity changes likely contributed more than mucilage dynamics to the dry-end responses observed; direct quantification of mucilage abundance and spatial distribution across genotypes will be needed to further test this hypothesis.

4.3. Implications for breeding and sustainable water use

These genotype-specific hydraulic responses have direct agronomic relevance. Root traits that help maintain soil porosity and hydraulic conductivity during soil drying may improve water-use efficiency, enhance drought resilience, and reduce irrigation demand, particularly in coarse-textured soils where plant-available water (PAW) is naturally limited (Ober et al., 2021). However, our results also reveal potential trade-offs. In some cases, increased water retention was associated with a higher permanent wilting point (PWP), which reduced the amount of plant-available water. These findings suggest that selecting crops solely for greater fine-root proliferation may not always lead to improved water availability for plants.

These results support the integration of root system architecture (RSA) traits into crop breeding and cropping system design (Ober et al., 2021; Zhang et al., 2025). However, the effects of genotype are strongly influenced by soil structure, management practices, and climatic conditions (Paez-Garcia et al., 2015; Uga, 2021).

The hydraulic improvements observed for the landrace Watkins 238 are noteworthy in this context. Modern wheat breeding has historically prioritised above-ground traits and rarely selected directly for root architecture (Voss-Fels et al., 2017), and the resulting genetic narrowing may have reduced the architectural diversity available to modulate rhizosphere hydraulic function. The Watkins bread-wheat collection (Wingen et al., 2014) and the broader Mediterranean durum landrace pool (Maccaferri et al., 2019) both offer structured platforms for re-introgressing landrace-derived root variation into elite germplasm, and our results suggest soil hydraulic functionality is one trait class for which this approach may be worth pursuing across both bread and durum wheat backgrounds.

4.4. Limitations and future directions

Although the experimental design provided sufficient power to detect genotype-associated differences in hydraulic behaviour, the relatively limited number of biological replicates means these findings should be interpreted as indicative rather than definitive and require validation across additional environments and seasons.

Furthermore, the observed relationships between root traits and hydraulic properties were inferred partly from pore-size distributions derived through hydraulic model parameterisation rather than direct structural observations. Future work combining high-resolution imaging approaches (e.g., X-ray CT or MRI), quantitative assessment of rhizosphere mucilage, and validation across contrasting soil types will be important for confirming the structural mechanisms underlying these genotype-specific hydraulic signatures and evaluating their stability under realistic agronomic conditions. Although high-resolution imaging techniques provide direct structural information, soil hydraulic measurements offer a scalable and comparatively cost-effective approach for assessing the functional impact of root–soil interactions across larger numbers of genotypes, soils, and environmental conditions. This makes hydraulic phenotyping a useful complement to structural approaches when evaluating genotype-dependent effects on soil water dynamics.

5. Conclusions

This study examined whether genotypic variation in wheat root system architecture influences soil pore structure and hydraulic behaviour under field conditions. The results show that contrasting genotypes modify rhizosphere pore architecture, leading to measurable differences in soil hydraulic properties, including water retention, plant-available water, and hydraulic conductivity during soil drying. Genotypes characterised by finer root diameters and architecturally complex root systems tended to generate bimodal pore size distributions and improved hydraulic performance under unsaturated conditions.

These findings suggest that root architectural traits can influence rhizosphere hydrological functioning by reshaping pore connectivity and pore size distribution. Integrating such traits into breeding strategies may therefore offer opportunities to improve soil–plant water relations and enhance crop resilience in water-limited environments.

CRediT authorship contribution statement

Bartolo Giuseppe Dimattia: Writing – review & editing, Writing – original draft, Visualization, Validation, Methodology, Data curation, Conceptualization. **Marco Bittelli:** Writing – review & editing, Supervision, Methodology, Conceptualization. **Fausto Tomei:** Software. **Roberto Tuberosa:** Writing – review & editing. **Maria C. Hernandez-Soriano:** Writing – review & editing, Resources, Funding acquisition.

Declaration of generative AI and AI-assisted technologies in the writing process

During the preparation of this work, the author used *Gemini (Google)* to improve the clarity and readability of the manuscript. After using this tool, the author reviewed and edited the content as needed and takes full responsibility for the content of the publication.

Declaration of competing interest

The authors declare that they have no known competing financial interests or personal relationships that could have appeared to influence the work reported in this paper.

Acknowledgements

B.G.D. received funding from the Department of Agricultural and Food Sciences (DISTAL), University of Bologna, Italy, through its Ph.D programme. M.C.H.S. gratefully acknowledges funding support from the Biotechnology and Biological Sciences Research Council (BBSRC), United Kingdom, project BB/X003000/1. We thank Silvio Salvi for useful discussion and for participation in the development and implementation of the funded project. We are also grateful to Marco Maccaferri for providing the seeds of the cultivar Senatore Cappelli and for useful discussions, to the John Innes Centre Germplasm Resources Unit for providing the seeds of the Paragon and Watkins 238 cultivars, and to Simon Griffiths and Luzie U. Wingen for advice on the relevance of these cultivars. B.G.D. gratefully acknowledges the support of the Collegio Superiore and the Institute of Advanced Studies of the University of Bologna. We would like to thank METER Group Inc. (Munich, Germany) where the measurements of the SHPs were performed, for providing access to the soil hydraulic instrumentation and Prof. Wolfgang Durner for generously sharing his expertise and guidance throughout the study.

Appendix A. Supplementary data

Supplementary data to this article provides additional methodological details, baseline soil properties, supplementary figures illustrating genotype selection and root image analysis, and a comprehensive description of the root morphological and soil hydraulic parameters used in this study. Supplementary data can be found online at https://doi.org/10.1016/j.geoderma.2026.117966.

Data availability

The computer code, written in Python and used to fit the bimodal model, is available upon request from the authors.

References

Ahuja, L.R., Naney, J.W., Williams, R.D., 1985. Estimating soil water characteristics from simpler properties or limited data. Soil Sci. Soc. Am. J. 49, 1100–1105.

Alexander, L., Skaggs, R., 1986. Predicting unsaturated hydraulic conductivity from the soil water characteristic. Trans. ASABE 29, 0176–0184.
Bardgett, R.D., Mommer, L., De Vries, F.T., 2014. Going underground: root traits as drivers of ecosystem processes. Trends Ecol. Evol. 29, 692–699.
Bengough, A.G., McKenzie, B.M., Hallett, P.D., Valentine, T.A., 2011. Root elongation, water stress, and mechanical impedance: a review of limiting stresses and beneficial root tip traits. J. Exp. Bot. 62, 59–68.
Bezerra-Coelho, C.R., Zhuang, L., Barbosa, M.C., Soto, M.A., van Genuchten, M.T., 2018. Further tests of the HYPROP evaporation method for estimating the unsaturated soil hydraulic properties. J. Hydrol. Hydromech./Vodohospo Cas 66, 161–169.
Bittelli, M., Campbell, G.S., Tomei, F., 2015. Soil physics with Python: transport in the soil-plant-atmosphere system. OUP Oxford.
Blanco-Canqui, H., Lal, R., Post, W., Izaurralde, R., Shipitalo, M., 2007. Soil hydraulic properties influenced by corn stover removal from no-till corn in Ohio. Soil Tillage Res. 92, 144–155.
Bodner, G., Leitner, D., Kaul, H.-P., 2014. Coarse and fine root plants affect pore size distributions differently. Plant and Soil 380, 133–151.
Bordoloi, R., Das, B., Yam, G., Pandey, P.K., Tripathi, O.P., 2019. Modeling of water holding capacity using readily available soil characteristics. Agric. Res. 8, 347–355.
Bronick, C.J., Lal, R., 2005. Soil structure and management: a review. Geoderma 124, 3–22.
Burden, R.L., Faires, J.D., 1997. Numerical analysis, brooks.
Campbell, G.S., Smith, D.M., Teare, B.L., 2007. Application of a dew point method to obtain the soil water characteristic. In: Springer Proceedings in Physics. Springer, Berlin Heidelberg, Berlin, Heidelberg, pp. 71–77.
Carminati, A., Moradi, A.B., Vetterlein, D., Vontobel, P., Lehmann, E., Weller, U., Vogel, H.-J., Oswald, S.E., 2010. Dynamics of soil water content in the rhizosphere. Plant and Soil 332, 163–176.
Carminati, A., Vetterlein, D., 2013. Plasticity of rhizosphere hydraulic properties as a key for efficient utilization of scarce resources. Ann. Bot. 112, 277–290.
Carminati, A., Zarebanadkouki, M., Kroener, E., Ahmed, M.A., Holz, M., 2016. Biophysical rhizosphere processes affecting root water uptake. Ann. Bot. 118, 561–571.
Corneo, P.E., Suenaga, H., Kertesz, M.A., Dijkstra, F.A., 2016. Effect of twenty four wheat genotypes on soil biochemical and microbial properties. Plant and Soil 404, 141–155.
Daly, K.R., Mooney, S.J., Bennett, M.J., Crout, N.M.J., Roose, T., Tracy, S.R., 2015. Assessing the influence of the rhizosphere on soil hydraulic properties using X-ray computed tomography and numerical modelling. J. Exp. Bot. 66, 2305–2314.
Dexter, A.R., 2004. Soil physical quality. Geoderma 120, 201–214.
Dimattia, B.G., Righi, A., Bettuzzi, M., Koestel, J., Morigi, M.P., Brancaccio, R., Salvi, S., Hernandez-Soriano, M.C., Bittelli, M., 2025. Root traits of different wheat cultivars influence soil structure: an X-ray computed tomography and root morphology study. Geoderma 459, 117349.
Doran, J.W., Parkin, T.B., 2015. Defining and assessing soil quality. In: SSSA Special Publications. Soil Science Society of America and American Society of Agronomy, Madison, WI, USA, pp. 1–21.
Durner, W., 1994. Hydraulic conductivity estimation for soils with heterogeneous pore structure. Water Resour. Res. https://doi.org/10.1029/93WR02676.
Evert, R.F., 2006. Esau's plant anatomy: meristems, cells, and tissues of the plant body: their structure, function, and development.
Fradgley, N., Evans, G., Biernaskie, J.M., Cockram, J., Marr, E.C., Oliver, A.G., Ober, E., Jones, H., 2020. Effects of breeding history and crop management on the root architecture of wheat. Plant and Soil 452, 587–600.
Freschet, G.T., Roumet, C., Comas, L.H., Weemstra, M., Bengough, A.G., Rewald, B., Bardgett, R.D., De Deyn, G.B., Johnson, D., Klimešová, J., Lukac, M., McCormack, M. L., Meier, I.C., Pagès, L., Poorter, H., Prieto, I., Wurzburger, N., Zadworny, M., Bagniewska-Zadworna, A., Blancaflor, E.B., Brunner, I., Gessler, A., Hobbie, S.E., Iversen, C.M., Mommer, L., Picon-Cochard, C., Postma, J.A., Rose, L., Ryser, P., Scherer-Lorenzen, M., Soudzilovskaia, N.A., Sun, T., Valverde-Barrantes, O.J., Weigelt, A., York, L.M., Stokes, A., 2021. Root traits as drivers of plant and ecosystem functioning: current understanding, pitfalls and future research needs. New Phytol. 232, 1123–1158.
Gregory, P.J. (Ed.), 2006. Plant roots: Growth, activity and interaction with soils. Wiley, Oxford, UK.
Grossman, J.D., Rice, K.J., 2012. Evolution of root plasticity responses to variation in soil nutrient distribution and concentration: barley root plasticity. Evol. Appl. 5, 850–857.
Hallett, P.D., Young, I.M., 1999. Changes to water repellence of soil aggregates caused by substrate-induced microbial activity. Eur. J. Soil Sci. 50, 35–40.
Hallett, P.D., Marin, M., Bending, G.D., George, T.S., Collins, C.D., Otten, W., 2022. Building soil sustainability from root-soil interface traits. Trends Plant Sci. 27, 688–698.
Helliwell, J.R., Sturrock, C.J., Mairhofer, S., Craigon, J., Ashton, R.W., Miller, A.J., Whalley, W.R., Mooney, S.J., 2017. The emergent rhizosphere: imaging the development of the porous architecture at the root-soil interface. Sci. Rep. 7, 14875.
Hodge, A., Berta, G., Doussan, C., Merchan, F., Crespi, M., 2009. Plant root growth, architecture and function. Plant and Soil 321, 153–187.
Hohenbrink, T.L., Jackisch, C., Durner, W., Germer, K., Iden, S.C., Kreiselmeier Peters, J., 2023. Soil water retention and hydraulic conductivity measured in a wide saturation range. Earth Syst. Sci. Data 15, 4417–4432.
Holz, M., Leue, M., Ahmed, M.A., Benard, P., Gerke, H.H., Carminati, A., 2018. Spatial distribution of mucilage in the rhizosphere measured with infrared spectroscopy. Front. Environ. Sci. 6. https://doi.org/10.3389/fenvs.2018.00087.
Jarvis, N.J., 2007. A review of non-equilibrium water flow and solute transport in soil macropores: principles, controlling factors and consequences for water quality. Eur. J. Soil Sci. 58, 523–546.
Jarvis, N.J., Messing, I., 1995. Near-saturated hydraulic conductivity in soils of contrasting texture measured by tension infiltrometers. Soil Sci. Soc. Am. J. 59, 27–34.
Jin, K., Shen, J., Ashton, R.W., Dodd, I.C., Parry, M.A.J., Whalley, W.R., 2013. How do roots elongate in a structured soil? J. Exp. Bot. 64, 4761–4777.
Jin, K., White, P.J., Whalley, W.R., Shen, J., Shi, L., 2017. Shaping an optimal soil by root–soil interaction. Trends Plant Sci. 22, 823–829.
Klute, A., Dirksen, C., 2018. Hydraulic conductivity and diffusivity: laboratory methods, in: SSSA Book Series. Soil Science Society of America, American Society of Agronomy, Madison, WI, USA, pp. 687–734.
Koebernick, N., Daly, K.R., Keyes, S.D., Bengough, A.G., Brown, L.K., Cooper, L.J., George, T.S., Hallett, P.D., Naveed, M., Raffan, A., Roose, T., 2019. Imaging microstructure of the barley rhizosphere: particle packing and root hair influences. New Phytol. 221, 1878–1889.
Kroener, E., Holz, M., Zarebanadkouki, M., Ahmed, M., Carminati, A., 2018. Effects of mucilage on rhizosphere hydraulic functions depend on soil particle size. Vadose Zone J. 17, 1–11.
Le Marié, C.A., York, L.M., Strigens, A., Malosetti, M., Camp, K.-H., Giuliani, S., Lynch, J. P., Hund, A., 2019. Shovelomics root traits assessed on the EURoot maize panel are highly heritable across environments but show low genotype-by-nitrogen interaction. Euphytica 215. https://doi.org/10.1007/s10681-019-2472-8.
Liu, H., Lennartz, B., 2019. Hydraulic properties of peat soils along a bulk density gradient—a meta study. Hydrol. Process. 33, 101–114.
Lu, J., Zhang, Q., Werner, A.D., Li, Y., Jiang, S., Tan, Z., 2020. Root-induced changes of soil hydraulic properties – a review. J. Hydrol. (amst.) 589, 125203.
Lucas, M., Schlüter, S., Vogel, H.-J., Vetterlein, D., 2019. Roots compact the surrounding soil depending on the structures they encounter. Sci. Rep. 9, 16236.
Lynch, J., 1995. Root architecture and plant productivity. Plant Physiol. 109, 7–13.
Maccaferri, M., Harris, N.S., Twardziok, S.O., Pasam, R.K., Gundlach, H., Spannagl, M., Ormanbekova, D., Lux, T., Prade, V.M., Milner, S.G., Himmelbach, A., Mascher, M., Bagnaresi, P., Faccioli, P., Cozzi, P., Lauria, M., Lazzari, B., Stella, A., Manconi, A., Gnocchi, M., Moscatelli, M., Avni, R., Deek, J., Biyiklioglu, S., Frascaroli, E., Corneti, S., Salvi, S., Sonnante, G., Desiderio, F., Marè, C., Crosatti, C., Mica, E., Özkan, H., Kilian, B., De Vita, P., Marone, D., Joukhadar, R., Mazzucotelli, E., Nigro, D., Gadaleta, A., Chao, S., Faris, J.D., Melo, A.T.O., Pumphrey, M., Pecchioni, N., Milanesi, L., Wiebe, K., Ens, J., MacLachlan, R.P., Clarke, J.M., Sharpe, A.G., Koh, C.S., Liang, K.Y.H., Taylor, G.J., Knox, R., Budak, H., Mastrangelo, A.M., Xu, S.S., Stein, N., Hale, I., Distelfeld, A., Hayden, M.J., Tuberosa, R., Walkowiak, S., Mayer, K.F.X., Ceriotti, A., Pozniak, C.J., Cattivelli, L., 2019. Durum wheat genome highlights past domestication signatures and future improvement targets. Nat. Genet. 51, 885–895.
Marshall, T.J., Holmes, J.W., Rose, C.W., 1996. Soil Physics, 3rd ed. Cambridge University Press, Cambridge, England.
Mualem, Y., 1976. A new model for predicting the hydraulic conductivity of unsaturated porous media. Water Resour. Res. 12, 513–522.
Naveed, M., Ahmed, M.A., Benard, P., Brown, L.K., George, T.S., Bengough, A.G., Roose, T., Koebernick, N., Hallett, P.D., 2019. Surface tension, rheology and hydrophobicity of rhizodeposits and seed mucilage influence soil water retention and hysteresis. Plant and Soil 437, 65–81.
Ober, E.S., Alahmad, S., Cockram, J., Forestan, C., Hickey, L.T., Kant, J., Maccaferri, M., Marr, E., Milner, M., Pinto, F., Rambla, C., Reynolds, M., Salvi, S., Sciara, G., Snowdon, R.J., Thomelin, P., Tuberosa, R., Uauy, C., Voss-Fels, K.P., Wallington, E., Watt, M., 2021. Wheat root systems as a breeding target for climate resilience. Theor. Appl. Genet. 134, 1645–1662.
Paez-Garcia, A., Motes, C.M., Scheible, W.-R., Chen, R., Blancaflor, E.B., Monteros, M.J., 2015. Root traits and phenotyping strategies for plant improvement. Plants 4, 334–355.
Peters, A., Durner, W., 2008. Simplified evaporation method for determining soil hydraulic properties. J. Hydrol. (amst.) 356, 147–162.
Rabot, E., Wiesmeier, M., Schlüter, S., Vogel, H.-J., 2018. Soil structure as an indicator of soil functions: a review. Geoderma 314, 122–137.
Rawls, W.J., Gimenez, D., Grossman, R., 1998. Use of soil texture, bulk density, and slope of the water retention curve to predict saturated hydraulic conductivity. Trans. ASAE 41, 983–988.
Schaap, M.G., van Genuchten, M.T., 2006. A modified Mualem–van Genuchten formulation for improved description of the hydraulic conductivity near saturation. Vadose Zone J. 5, 27–34.
Schindler, U., Durner, W., von Unold, G., Mueller, L., Wieland, R., 2010. The evaporation method: extending the measurement range of soil hydraulic properties using the air-entry pressure of the ceramic cup. J. Plant Nutr. Soil Sci. 173, 563–572.
Scholl, P., Leitner, D., Kammerer, G., Loiskandl, W., Kaul, H.-P., Bodner, G., 2014. Root induced changes of effective 1D hydraulic properties in a soil column. Plant and Soil 381, 193–213.
Seethepalli, A., Dhakal, K., Griffiths, M., Guo, H., Freschet, G.T., York, L.M., 2021. RhizoVision Explorer: open-source software for root image analysis and measurement standardization. AoB Plants 13 (6), plab056.
Seki, K., Toride, N., van Genuchten, Th., 2022. Closed-form hydraulic conductivity equations for multimodal unsaturated soil hydraulic properties. Vadose Zone J. 21. https://doi.org/10.1002/vzj2.20168.
Šimůnek, J., Brunetti, G., Jacques, D., van Genuchten, M.T., Šejna, M., 2024. Developments and applications of the HYDRUS computer software packages since 2016. Vadose Zone J. 23. https://doi.org/10.1002/vzj2.20310.

Singh, A., Verdi, A., 2024. Estimating the soil water retention curve by the HYPROP-WP4C system, HYPROP-based PCNN-PTF and inverse modeling using HYDRUS-1D. J. Hydrol. (amst.) 639, 131657.
Staszel-Szlachta, K., Lasota, J., Szlachta, A., Błońska, E., 2024. The impact of root systems and their exudates in different tree species on soil properties and microorganisms in a temperate forest ecosystem. BMC Plant Biol. 24, 45.
Strudley, M., Green, T., Ascoughii, J., 2008. Tillage effects on soil hydraulic properties in space and time: state of the science. Soil Tillage Res. 99, 4–48.
Trachsel, S., Kaeppler, S.M., Brown, K.M., Lynch, J.P., 2011. Shovelomics: high throughput phenotyping of maize (*Zea mays* L.) root architecture in the field. Plant and Soil 341, 75–87.
Tuller, M., Or, D., Dudley, L.M., 1999. Adsorption and capillary condensation in porous media: liquid retention and interfacial configurations in angular pores. Water Resour. Res. 35, 1949–1964.
Uga, Y., 2021. Challenges to design-oriented breeding of root system architecture adapted to climate change. Breed. Sci. 71, 3–12.
van Genuchten, M.T., 1980. A closed-form equation for predicting the hydraulic conductivity of unsaturated soils. Soil Sci. Soc. Am. J. 44, 892–898.
van Genuchten, M., Leij, F., Yates, S., 1992. The RETC code for quantifying the hydraulic functions of unsaturated soils.
Voss-Fels, K.P., Qian, L., Parra-Londono, S., Uptmoor, R., Frisch, M., Keeble-Gagnère, G., Appels, R., Snowdon, R.J., 2017. Linkage drag constrains the roots of modern wheat. Plant Cell Environ. 40 (5), 717–725.
Wang, P., Ding, L., Zou, C., Zhang, Y., Wang, M., 2022. Rhizosphere element circling, multifunctionality, aboveground productivity and trade-offs are better predicted by rhizosphere rare taxa. Front. Plant Sci. 13, 985574.
White, C.A., Sylvester-Bradley, R., Berry, P.M., 2015. Root length densities of UK wheat and oilseed rape crops with implications for water capture and yield. J. Exp. Bot. 66, 2293–2303.
Wind, G.P., 1968. Capillary conductivity data estimated by a simple method. Water in the Unsaturated Zone 1, 181–191.
Wingen, L.U., Orford, S., Goram, R., Leverington-Waite, M., Bilham, L., Patsiou, T.S., Ambrose, M., Dicks, J., Griffiths, S., 2014. Establishing the a. E. Watkins landrace cultivar collection as a resource for systematic gene discovery in bread wheat. Züchter Genet. Breed. Res. 127, 1831–1842.
Xiao, T., Li, P., Fei, W., Wang, J., 2024. Effects of vegetation roots on the structure and hydraulic properties of soils: a perspective review. Sci. Total Environ. 906, 167524.
York, L.M., Slack, S., Bennett, M.J., Foulkes, M.J., 2018. Wheat shovelomics I: a field phenotyping approach for characterising the structure and function of root systems in tillering species. bioRxiv. https://doi.org/10.1101/280875.
Young, I.M., Ritz, K., 2005. The habitat of soil microbes. https://doi.org/10.5555/20073109422.
Zhang, Y., Wu, X., Wang, X., Dai, M., Peng, Y., 2025. Crop root system architecture in drought response. J. Genet. Genomics 52, 4–13.
Zhou, H., Whalley, W.R., Hawkesford, M.J., Ashton, R.W., Atkinson, B., Atkinson, J.A., Sturrock, C.J., Bennett, M.J., Mooney, S.J., 2021. The interaction between wheat roots and soil pores in structured field soil. J. Exp. Bot. 72, 747–756.